Magnetic moment of the 4_1^+ state in ^{20}Ne

T. Bright,* D. Ballon, R. J. Saxena,† Y. Niv, and N. Benczer-Koller
Department of Physics, Rutgers University, New Brunswick, New Jersey 08903
(Received 15 March 1984)

The magnetic moment of the 4_1^+ state in ^{20}Ne was measured by the transient field technique, and the transient field was calibrated in a simultaneous measurement on the 2_1^+ state. The resulting $g(4_1^+)=0.49\pm0.34$ is in agreement with the shell model description of ^{20}Ne. The magnitude of the transient field measured in previous experiments on O, Ne, and Mg ions traversing iron foils was reexamined and appears to be in good agreement with the results of this experiment.

I. INTRODUCTION

The magnetic moment of the 4_1^+ (4.25 MeV, 93 fs) state of ^{20}Ne has been recently measured by the transient field technique by Speidel *et al.*[1,2] Two separate measurements on ^{20}Ne ions recoiling through thin iron and gadolinium foils have yielded $g=-0.10(14)$ and $+0.08(20)$, respectively. These results are in complete disagreement with the predictions of shell-model calculations. The structure of ^{20}Ne has been extensively studied, and it is expected that the g factor of pure $T=0$ states in self-conjugate nuclei would be in the range $0.45\leq g_{\rm th}\leq 0.55$. Recent calculations[3] for $N=Z$ nuclei which include isospin mixing also fail to reproduce the vanishingly small experimental magnetic moment. Moreover, measurements of the magnetic moments of low lying states in nearby nuclei [^{24}Mg(2_1^+) (Ref. 4) and ^{24}Mg(4_1^+) (Ref. 5), ^{20}Ne(2_1^+) (Ref. 4), and ^{16}O(3_1^-) (Ref. 6)] have confirmed the shell-model predictions. The experimental result for $g(^{20}\text{Ne},4_1^+)$ was therefore attributed to the contribution from a partial alignment of decoupled neutrons in $j=1+\frac{1}{2}$ orbitals in the s-d shell. The same mechanism is thought to be responsible for the backbending phenomena in deformed nuclei. In fact, it has been suggested that the low lying levels of ^{20,22}Ne do show collective structure and, furthermore, that their pattern deviates markedly from a pure rotational sequence at the 6_1^+ state.[7] In spite of this evidence, the view that the 4_1^+ state already exhibits backbending properties is not in agreement with any current wisdom.

In view of the fundamental importance of the structure of the low lying levels of ^{20}Ne to the understanding of the residual interactions in light nuclei, experiments similar to those of Speidel *et al.* were undertaken. The transient fields experienced by fast ions traversing magnetic materials have the advantage of being very large; however, the technique suffers from serious uncertainties in the calibration of the transient field. In the published measurements on $g(^{20}\text{Ne},4_1^+)$, the precession of the angular correlation pattern of the decay gamma rays $\underline{4_1^+\rightarrow 2_1^+}$ and $4_1^+\rightarrow\underline{2_1^+\rightarrow 0_1^+}$ were compared to each other, while the magnetic moment of the 2_1^+ state (1.67 MeV, 1.05 ps), $g=0.54(4)$, obtained previously in time differential recoil-into-vacuum experiments,[4] was used as a standard. A direct calibration of the transient field on the directly excited 2_1^+ state was carried out in the case of recoil through iron.[1] In the latter experiment on ^{20}Ne ions recoiling through gadolinium,[2] only the cascade transitions were measured.

In the work reported here, the experimental conditions were similar to those of Speidel *et al.*, but both the 4_1^+ state and the 2_1^+ state were studied separately, and the transient field strength was reanalyzed as a free parameter. A reevaluation of the transient field data in neighboring nuclei O and Mg was carried out in order to obtain a consistent estimate of the magnitude of the transient field in light nuclei.

II. EXPERIMENTAL PROCEDURES

A. Geometrical layout, targets, and magnetization measurements

The general layout of the experimental setup is shown in Fig. 1. The states in ^{20}Ne were excited in the reaction ^{12}C(^{12}C,α)^{20}Ne*, with the ^{12}C beam from the Rutgers-Bell Tandem Van de Graaff. The α particles were detected by an annular surface barrier detector subtending an angle between 165° and 172° to the beam direction. Backscattered particle spectra at beam energies corresponding to maximum resonance excitation of the 4_1^+ [$E(^{12}\text{C})=32.3$ MeV] and 2_1^+ [$E(^{12}\text{C})=34.7$ MeV] states, respectively, are shown in Figs. 2(a) and (b).

The decay gamma radiation was detected in coincidence with the backscattered particles in four 12.7 cm×12.7 cm NaI(Tl) detectors located 16.7 cm away from the target, positioned either at ±65° and ±115° (2_1^+ excitation) or at ±60° and ±120° (4_1^+ excitation), the angles at which the α-γ coincidence gamma ray angular distribution $W(\theta)$ exhibits its maximum logarithmic slope $S=(1/W)(dW/d\theta)$.

The target consisted of a 105 μg/cm^2 thick ^{12}C layer evaporated onto a 2.77 mg/cm^2 thick natural gadolinium foil backed by 15 mg/cm^2 of copper. The magnetization of the target was measured before and after each run as a function of temperature in a double coil compensation magnetometer.[8] A magnetization of $M=0.1524(46)$ T was determined in an external field of 0.045 T at 120 K. This value of magnetization corresponds to 5.4 polarized electrons per atom.

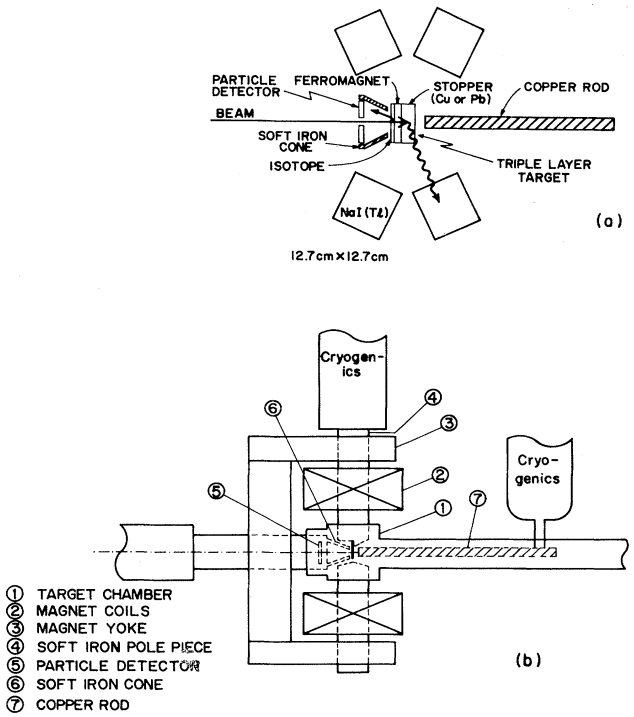

FIG. 1. (a) Schematic diagram of the experimental arrangement. (b) Detail of the magnet chamber and cryogenic devices.

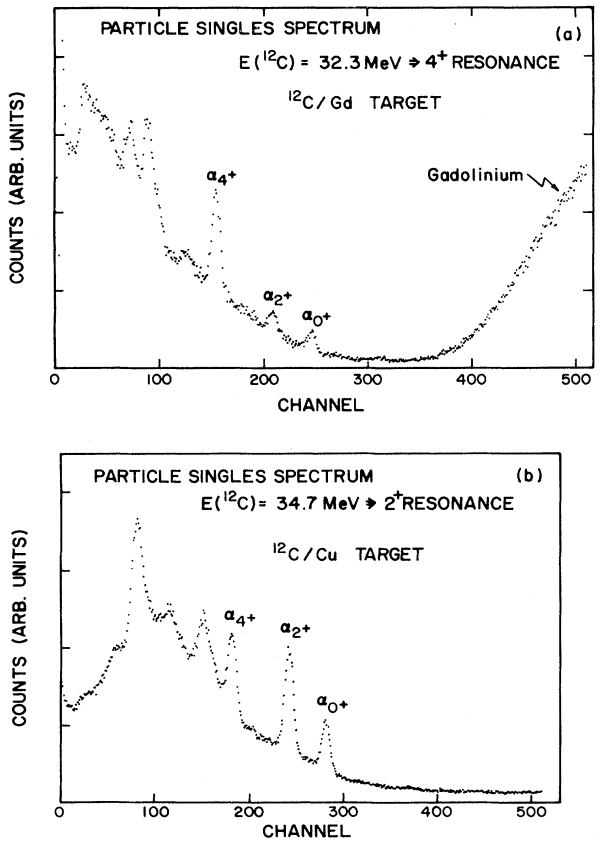

FIG. 2. Typical energy spectra of backscattered α particles for incident C energies of (a) $E(^{12}C)=32.3$ MeV and (b) $E(^{12}C)=34.7$ MeV.

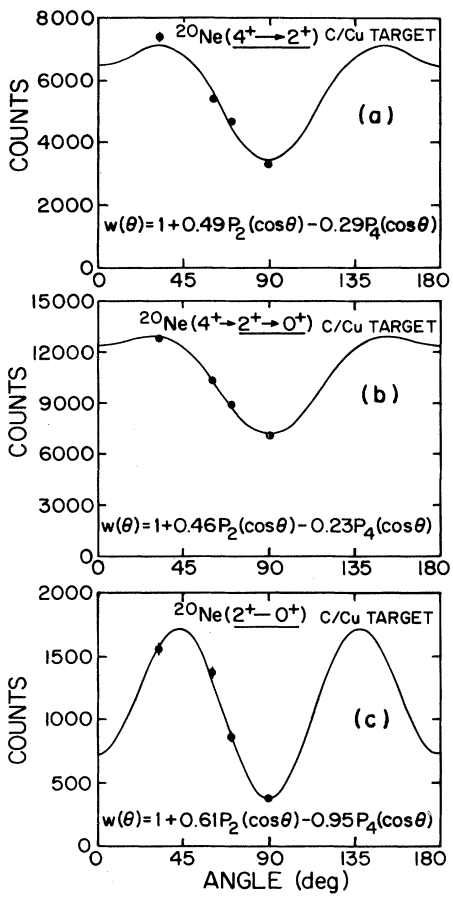

FIG. 3. α-γ angular correlations obtained with a C/Cu target for the three transitions (a) $4_1^+ \rightarrow 2_1^+$, (b) $4_1^+ \rightarrow 2_1^+ \rightarrow 0_1^+$, and (c) $2_1^+ \rightarrow 0_1^+$.

The target was thermally attached to the upper pole piece of an electromagnet which is part of a cryogenic compressor unit. The cold tip was maintained at 120 K. At lower temperatures a considerable amount of residual gases condensed on the target, resulting in reactions leading to ^{24}Mg*, which exhibits a gamma ray spectrum similar to that of ^{20}Ne*. A long copper rod thermally attached to a liquid nitrogen Dewar was placed immediately behind the target. This additional cold trap improved the vacuum in the interaction region and essentially eliminated condensation of impurities on the target.

The direction of the magnetic field produced by the electromagnet was switched regularly, approximately every 10 min, after accumulation of a preset number of counts of backscattered α particles. In order to minimize stray magnetic fields in the scattering region, a soft magnetic core was positioned around the path of the incoming beam between the particle detector and the target.

The precession of the angular correlation pattern caused by the bending of the incoming and scattered particles in the stray magnetic field surrounding the magnet pole pieces was measured separately under the same geometrical conditions as used for the magnetic moment measurements, on a target consisting of 165 μg/cm^2 of ^{12}C evaporated directly on a 22 mg/cm^2 copper foil.

Three types of experiments were carried out at the two incident beam energies where the two states of interest are predominantly excited: gamma ray angular distributions (Fig. 3), beam bending measurements using the nonmagnetic target, and precession determinations on the gadolinium target.

B. Spectral analysis

The gamma ray spectra were systematically analyzed in a sequence of steps. First, the random coincidence spectra were subtracted from the total spectra. The high energy background portion was then fitted to a constant and subtracted from the spectra. This procedure yields clear spectra of the $4_1^+ \rightarrow 2_1^+$ and $2_1^+ \rightarrow 0_1^+$ (direct excitation) radiations. The $4_1^+ \rightarrow 2_1^+$ intensity included the photopeak, the Compton, and the single escape peak, but excluded the region below 2 MeV which contains the cascade $4_1^+ \rightarrow 2_1^+ \rightarrow 0_1^+$ radiation.

In order to analyze the cascade radiation, a ^{228}Th source was placed in the target position, and a singles gamma spectrum was obtained. The high energy portion ($1.6 \lesssim E_\gamma \lesssim 3$ MeV) of this spectrum is very similar to that of the ^{20}Ne, $4_1^+ \rightarrow 2_1^+$, 2.63 MeV decay, except for the relatively worse detector resolution for the in-beam measurements. Therefore, the ^{228}Th spectrum was convoluted with a Gaussian distribution in order to produce a spectrum matching in width and intensity the in-beam spectrum in the region of the 2.63 MeV photopeak [Fig. 4(a)]; this convoluted spectrum was subtracted from the net coincidence spectrum (obtained by first subtracting the random spectrum from the total coincidence rate) to yield the portion of the spectrum corresponding to the cascade radiation at 1.67 MeV [Fig. 4(b)]. An analysis of the data carried out by estimating the background from its value just above the 1.67 MeV photopeak resulted in precessions of almost a factor of 2 larger than those obtained by the above method.

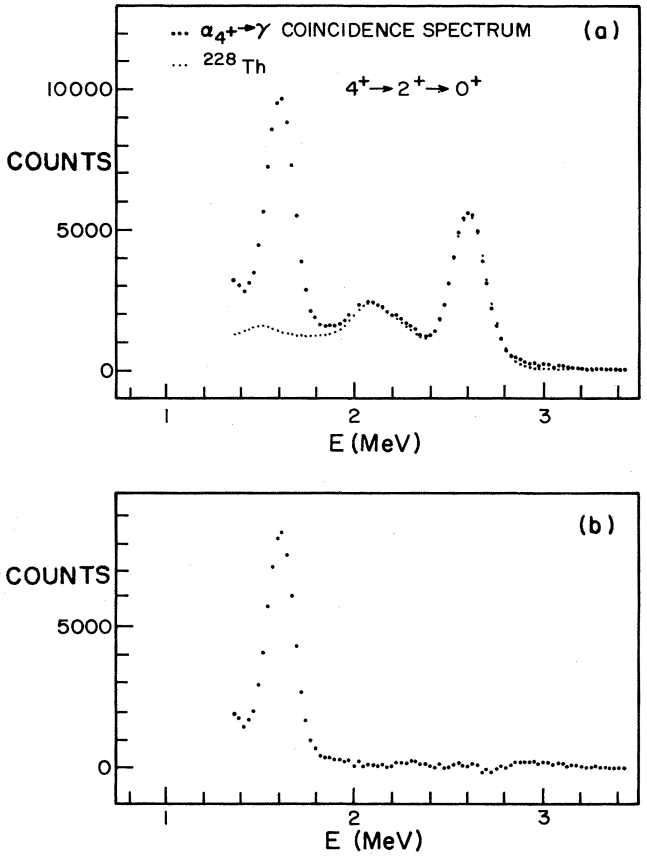

FIG. 4. (a) Comparison of the α_{4^+}-γ coincidence spectrum with the spectrum from a ^{228}Th source. (b) Spectrum of the cascade $4_1^+ \rightarrow 2_1^+ \rightarrow 0_1^+$ radiation after subtraction of the convoluted ^{228}Th spectrum [$\cdots$ in (a)].

C. Precession analysis

The net precession of the angular distribution under reversal of the external aligning magnetic field was analyzed

TABLE I. Experimental logarithmic derivatives $|S|$ of the gamma ray angular distributions observed with targets of carbon/gadolinium/copper and carbon/copper [used for beam bending (bb) measurements] and measured angular precessions.

	$\lvert S \rvert$ (gadolinium)	$-\Delta\theta$ (mrad)	$\lvert S_{bb} \rvert$ (copper)	$-\Delta\theta_{bb}$ (mrad)
	Optimized excitation of the 4_1^+ state:		$E(^{12}C)=32.3$ MeV	
$4_1^+ \rightarrow 2_1^+$	0.895(23)	1.17(158)	0.889(14)	0.43(107)
$4_1^+ \rightarrow 2_1^+ \rightarrow 0_1^+$	0.895(23)	6.15(180)	0.889(14)	0.43(107)
$2_1^+ \rightarrow 0_1^+$	1.749(113)	4.69(350)	1.697(59)	0.53(188)
	Optimized excitation of the 2_1^+ state:		$E(^{12}C)=34.7$ MeV	
$4_1^+ \rightarrow 2_1^+$	1.038(33)	4.12(284)	0.988(34)	3.54(203)
$4_1^+ \rightarrow 2_1^+ \rightarrow 0_1^+$	1.038(33)	7.71(463)	0.988(34)	3.54(203)
$2_1^+ \rightarrow 0_1^+$	1.751(36)	5.27(148)	1.662(46)	3.53(120)

TABLE II. Experimental net angular precessions observed for the three transitions in ^{20}Ne and comparison with the results of Speidel *et al.* (Ref. 2).

Transition	$E(^{12}C)$ (MeV)	$E(^{20}Ne)_{in}$ (MeV)	$\left[\frac{v}{v_0}\right]_{in}$	$\left[\frac{v}{v_0}\right]_{out}$	This work $-\Delta\theta$ (mrad)	This work $-\Delta\theta$ (mrad)	Ref. 2 $-\Delta\theta$ (mrad)
$4_1^+ \rightarrow 2_1^+$	32.3	27.5	7.43	a	0.74(191)	0.70(168)	0.46(114)
	34.7	29.6	7.72	a	0.58(349)		
$4_1^+ \rightarrow 2_1^+ \rightarrow 0_1^+$	32.3	27.5	7.43	5.77	5.72(209)	5.49(193)	6.08(112)
	34.7	29.6	7.72	6.14	4.17(505)		
$2_1^+ \rightarrow 0_1^+$	32.3	28.8	7.62	6.01	4.16(397)	2.19(172)	
	34.7	31.0	7.90	6.36	1.74(191)		

[a]The 4_1^+ state decays in flight in the gadolinium.

using the standard analysis technique described previously.[9,10] The ratios

$$\rho_{ij}=\left[\frac{N_i^{\uparrow}}{N_j^{\uparrow}}\Big/\frac{N_i^{\downarrow}}{N_j^{\downarrow}}\right]^{1/2}$$

were calculated. The subscripts $i,j=1$–4 represent the four detectors. $N_i^{\uparrow(\downarrow)}$ is the random- and background-subtracted field up (down) coincidence counting rate in the ith detector. The rotation $\Delta\theta$ of the angular distribution was obtained from the measured effect $\epsilon=\rho-1/\rho+1$, where $\rho=\sqrt{\rho_{14}/\rho_{23}}$ and $\Delta\theta=\epsilon/S$. The cross ratios $\rho_c=\sqrt{\rho_{13}/\rho_{24}}$, which should be unity if no systematic asymmetries are present, were continuously monitored.

The resulting precessions obtained by this procedure are displayed in Table I. Note that the relatively large beam bending measured at the higher beam energy $E(^{12}C)=34.7$ MeV is probably due to the strong resonance behavior of the reaction.[4] The net precessions obtained after subtraction of the beam bending are presented in Table II.

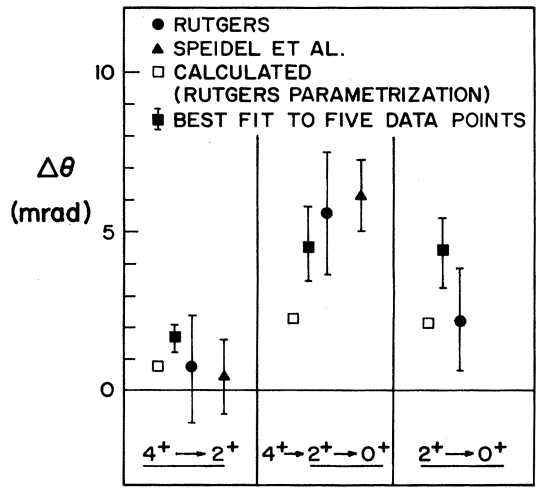

FIG. 5. Measured and calculated precessions for the three gamma ray transitions observed.

These results can be directly compared with those of Speidel *et al.* because the target thicknesses and beam energies were very close in both experiments. Figure 5 compares the net precession obtained in the present experiment with the results of Speidel *et al.* and with the precessions calculated by the method described in Sec. III. The measurements reported here are in good agreement with the data of Speidel *et al.*

III. RESULTS

A. Calculations of angular precessions

In order to extract the magnetic moment from the experimental precessions of the angular distribution, a model of the transient hyperfine fields must be adopted. In what follows the Rutgers parametrization of the field,[11]

$$\vec{B}_R(v,Z)=96.7(v/v_0)^{0.45}Z^{1.1}\vec{M}\ ,$$

was used. However, in the last stage of the analysis, described in Sec. III B, the magnitude of the transient field will be left as a free parameter.

The precession of the gamma ray angular distribution can be calculated from the following expressions:

$$\Delta\theta=\frac{\int\delta\theta\,dN}{\int dN}$$

and

$$\delta\theta=-g\frac{\mu_N}{\hbar}\int B(v,Z)dt\ ,$$

where dN is the population distribution of the state of in-

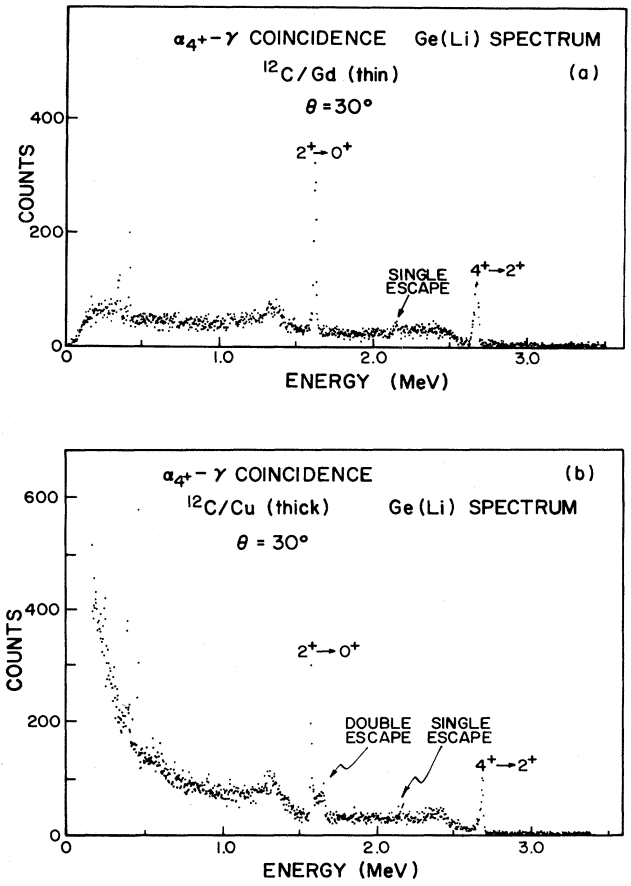

FIG. 6. α_{4^+}-γ coincidence spectra observed with a Ge(Li) detector at 30° with respect to the beam direction with (a) a thin C/gadolinium target such that only decays in flight occur; (b) a thick C/gadolinium/copper target such that the 4_1^+ state decays in flight but the 2_1^+ state stops before decaying. No radiations other than the two gamma rays from ^{20}Ne are observed at a level greater than 5%.

terest. The exact expressions appropriate for each transition are given in the Appendix.

The results of these calculations $\Delta\theta_{\text{calc}}$, assuming that $g(4_1^+)=0.5$ and $g(2_1^+)=0.54$, and the transient field $B_R(v,Z)$ are indicated by hollow squares in Fig. 5. Whereas the direct $4_1\rightarrow 2_1$ and $2_1\rightarrow 0_1$ transitions are well reproduced, it is clear that the precession of the cascade transition is larger than predicted.

It was thought that the larger precession observed in the cascade transition might be caused by an unresolved impurity radiation. Gamma-ray spectra were obtained with a Ge(Li) detector at 30°, in singles and coincidence modes, with the triple layer target and with a C/gadolinium target without the copper stopping layer. In this last configuration, the coincidence Ne recoils do not stop, and all radiations emitted at 30° are Doppler shifted towards higher energies, allowing inspection of the spectra in the region of radiation from stopped ions. No gamma ray lines other than those corresponding to ^{20}Ne were observed (Fig. 6).

B. Simultaneous fit of the data to both the transient hyperfine magnetic field and $g(4_1^+)$

1. Measurements on C/gadolinium/copper targets

In order to determine the magnetic moment of the 4_1^+ state with the least dependence on the model used for the transient field parametrization, the following procedure was followed:

There are three independent data points, the net precessions for the three transitions $4_1^+\rightarrow 2_1^+$, $4_1^+\rightarrow 2_1^+\rightarrow 0_1^+$, and $2_1^+\rightarrow 0_1^+$, and two unknown quantities: $g(4_1^+)$ and the amplitude of the hyperfine field $B(v,Z)$ to be approximated by $B(v,Z)=aB_R(v,Z)$. The three independent data points obtained in the present experiment can be plotted with the help of the formulae developed in the Appendix on a two-dimensional graph [Fig. 7(a)] of the unknown amplitude a vs the unknown magnetic moment $g(4_1^+)$. For every a and g, the chi-squared

$$\chi^2(a,g)=\sum_i\{[\Delta\theta_{i_{\text{exp}}}-\Delta\theta_{i_{\text{calc}}}(a,g)]/\sigma_{i_{\text{exp}}}\}^2$$

was computed where the sum i runs over the measurements of the three transitions considered and σ_{exp} is the statistical error in the measured precession $\Delta\theta_{\text{exp}}$. The point of minimum χ^2 yields the best simultaneous fit to both a and g, and the errors in these quantities were determined by calculating the appropriate covariance matrix. The best fit to the present data yields

$$a=1.3(7);\quad g(4_1^+)=+0.87(90)\ .$$

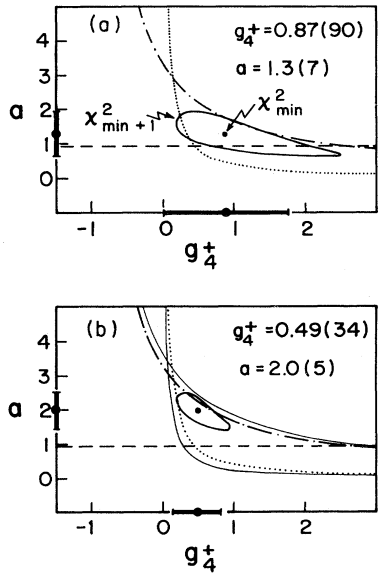

FIG. 7. Plot of the amplitude parameter a vs $g(4_1^+)$ for (a) the three data points obtained in this work and (b) these data as well as those of Speidel *et al.* (Ref. 2). The lines represent the following transitions: (···) $4_1^+\rightarrow 2_1^+\rightarrow 0_1^+$; (—·—·—·) $4_1^+\rightarrow 2_1^+$; (— — —) $2_1^+\rightarrow 0_1^+$; (——) Speidel *et al.* data. The value of a and $g(4_1^+)$ for which χ^2 is a minimum is indicated. The curve represents the locus of points with $\chi^2=\chi^2_{\text{min}}+1$.

The position of the minimum χ^2 (1.3 for one degree of freedom) is shown in Fig. 7(a) together with the locus of points $\chi^2=\chi^2_{\min}+1$.

Extending this procedure to include the data of Speidel *et al.*[2] yields

$$a=2.0(5);\quad g(4_1^+)=+0.43(34)\ ,$$

with $\chi^2_{\min}=4.6$ for three degrees of freedom. In Fig. 7(b) the combination of the three data points of this measurement, together with the two data points of Speidel *et al.*[2] are depicted, as well as the position of $\chi^2_{\min}$ and the locus of points $\chi^2=\chi^2_{\min}+1$. The filled squares in Fig. 5 represent the values of the precessions calculated for $a=2.0$, the best fit to the amplitude parameter.

2. *Experiments on C/iron/copper targets*

In early experiments on a C/iron/copper target, we found that the background in the particle and gamma-ray spectra was considerably larger than in the carbon on gadolinium experiments, rendering the analysis much less reliable. Speidel *et al.* were actually able to reduce the background in their measurements on C/iron targets by operating the particle detector at a low bias of less than 5 V. In these experiments, they also measured the precession of the decay radiation of the directly excited 2_1^+ state. The net precession expected for these measurements was *calculated* for $g(2_1^+)=0.54$ and $g(4_1^+)=0.5$ and a transient hyperfine field strength factor $a=2.0$, yielding $\Delta\theta(\underline{2^+\rightarrow 0^+})=3.26$ mrad, $\Delta\theta(4^+\rightarrow\underline{2^+\rightarrow 0^+})=3.36$ mrad, and $\Delta\theta(\underline{4^+\rightarrow 2^+})=1.40$ mrad, in fair agreement with the measured precessions,[12] 3.3(1.1), 2.7(0.5), and $-0.30(0.6)$ mrad, respectively. However, because of the possibility that the transient fields at Ne ions traversing iron and gadolinium foils are intrinsically different, the data on the C/iron/copper targets were not averaged with the data from the C/gadolinium/copper targets to determine the final result.

IV. DISCUSSION

The shortcomings of many experiments in hyperfine interactions have always been caused by the difficulties encountered in absolute calibrations of the hyperfine fields. Speidel *et al.* described the transient field in terms of a microscopic model with reasonable but not measured parameters. In order to minimize the uncertainties in the field calibration, the magnetic moment was extracted from the ratios of the precessions of the two transitions $\underline{4_1^+\rightarrow 2_1^+}$ and $4_1^+\rightarrow\underline{2_1^+\rightarrow 0_1^+}$. This procedure is equivalent to a two-point calibration, which is very sensitive to the value of the individual experimental data. As shown in Fig. 7, the analysis of these two data points leads to a small value for the nuclear g factor $g\sim 0.1$, and a very high field, $a\sim 3.3$.

In this work, the analysis was extended to a free fit of three and five data points. The fact that an explicit velocity dependence of the transient fields was chosen does not affect the final results as long as all the measurements are obtained in a similar narrow velocity interval.

The present analysis yields, in addition to the magnetic moment, an estimate of the transient field at Ne ions recoiling through gadolinium in the velocity range $5.8\lesssim v/v_0\lesssim 7.9$. The resulting field is about a factor of 2

TABLE III. Comparison of the precessions calculated assuming the transient field is given by the Rutgers parametrization (Ref. 11) and the experimental precession observed for oxygen, neon, and magnesium ions traversing iron foils.

Nucleus, E I^π,τ	g	$\left[\frac{v}{v_0}\right]_{\text{in}}$	$\left[\frac{v}{v_0}\right]_{\text{out}}$	$-\Delta\theta_{\text{exp}}$ (mrad)	$-\Delta\theta_{\text{calc}}$[a] (mrad)	$a=\frac{\Delta\theta_{\text{exp}}}{\Delta\theta_{\text{calc}}}$	Ref.
Oxygen ions:							
^{16}O, 6.13 MeV	0.55(3)	4.51	2.87	2.15(58)	1.28(7)	1.7(5)	11
3_1^-, 26.6 ps	Ref. 6	8.04	6.73	2.4(11)	1.33(7)	1.8(8)	13
		8.04	2.92	5.4(13)	4.37(24)	1.2(3)	13
		3.0	1.8	1.22(20)[b]	0.88(5)	1.4(2)	12
		3.0	1.4	2.46(30)[b]	1.44(8)	1.7(2)	12
Neon ions:							
^{20}Ne, 1.67 MeV	0.54(4)	7.8	5.9	2.1(8)	1.78(13)	1.2(5)	14
2_1^+, 1.05 ps	Ref. 4	7.8	5.2	2.8(7)	2.31(17)	1.2(3)	14
		7.8	6.0	3.3(11)	1.63(12)	2.0(7)	1
^{22}Ne, 1.275 MeV	0.326(12)	2.0	1.1	0.99(12)	0.83(3)	1.2(2)	15
2_1^+, 5.2 ps	Ref. 16						
Magnesium ions:							
^{24}Mg, 1.37 MeV	0.51(2)	7.8	6.77	2.47(66)	1.23(5)	2.0(5)	5
2_1^+, 1.98 ps	Ref. 4	7.8	5.98	3.10(67)	2.11(8)	1.5(3)	5
		7.8	5.08	4.43(52)	3.03(12)	1.5(2)	5

[a]The error in the calculations reflects the uncertainty in the measured g factor.

[b]Measurement carried out on thick iron foil. The precessions were analyzed differentially as described in Ref. 11 in order to mimic the thin iron foil measurements.

larger than predicted by the parametrization[11] which was obtained from a fit to nuclei from ^{16}O to Sm. However, the errors quoted[11] for the parameters in $B_R(v,Z)$ are quite large, rendering a factor of 2 in actual field strength in the low Z region possible. The existing transient fields experiments on $^{16}O(3_1^-)$ (Refs. 11–13), $^{20}Ne(2_1^+)$ (Ref. 14), $^{22}Ne(2_1^+)$ (Ref. 15), and $^{24}Mg(2_1^+)$ (Ref. 5) ions traversing an iron matrix have been reexamined and are compared to the present results. Table III shows the experimentally determined precession angles $\Delta\theta_{exp}$, the precessions $\Delta\theta_{calc}$, calculated with the field parametrization $B_R(v,Z)$, and the ratio $a=\Delta\theta_{exp}/\Delta\theta_{calc}$. The strength parameter a varies between 1 and 2 pointing out again the importance of calibrating the hyperfine field on the same isotope and in the same experimental conditions as those used in the measurement of the unknown magnetic moment.

In summary, these estimates of the transient hyperfine fields at $^{16}O(3_1^-)$, $^{20}Ne(2_1^+)$, $^{22}Ne(2_1^+)$, and $^{24}Mg(2_1^+)$ recoiling through iron are entirely consistent with the data for $^{20}Ne(4_1^+)$ recoiling through gadolinium.

The low Z and short meanlife of the 4_1^+ state result in a small transient field, a correspondingly small angular precession, and a relatively large uncertainty which cannot easily be reduced with present techniques. We therefore conclude that the resulting $g[^{20}Ne(4_1^+)]=0.49(34)$ is in agreement with shell model expectations even though the experimental error is not small enough to permit a *critical* comparison with theoretical calculations.

ACKNOWLEDGMENTS

We would like to acknowledge Dr. R. Levy for participating in the early phase of this experiment, R. Klein for skillful target preparation, and D. Leidich, P. Vlahakis, and R. Darling for technical help. This work was supported in part by the National Science Foundation.

APPENDIX: FORMULATION OF THE PRECESSIONS OF THE GAMMA RAY ANGULAR CORRELATIONS RESULTING FROM THE INFLUENCE OF THE TRANSIENT FIELD $B(v,Z)$

The precessions of the gamma ray angular correlations of the three transitions available in the decay of ^{20}Ne can be calculated from the formulae given below. The notation describing the time scale is shown in Fig. 8. The time $t=0$ is defined as the time at which the beam is incident on the carbon layer. The time $t=t^*$ is taken as the mean of the time of flight of the carbon projectile and neon fragments through the carbon layer. The Ne nuclei leave the ferromagnetic material at $t=t_s$. The precessions $\Delta\theta$ can be then formulated as follows:[17]

$$\Delta\theta(\underline{4^+\rightarrow 2^+})=-\frac{g_4\mu_N}{\hbar}\frac{\tau_4}{t^*}(e^{t^*/\tau_4}-1)\int_{t^*}^{t_s}B(v,Z)e^{-t/\tau_4}dt\equiv g_4\theta_4\ ,$$

$$\Delta\theta(\underline{2^+\rightarrow 0^+})=-\frac{g_2\mu_N}{\hbar}\frac{\tau_2}{t^*}(e^{t^*/\tau_2}-1)\int_{t^*}^{t_s}B(v,Z)e^{-t/\tau_2}dt\equiv g_2\theta_2\ ,$$

and

$$\Delta\theta(4^+\rightarrow\underline{2^+\rightarrow 0^+})=\Delta\theta(\underline{4^+\rightarrow 2^+})-\frac{\mu_N g_2\tau_2}{\hbar t^*(\tau_2-\tau_4)}\left[\tau_4(e^{t^*/\tau_4}-1)\int_{t^*}^{t_s}e^{-t/\tau_4}B(v,Z)dt+\tau_2(e^{t^*/\tau_2}-1)\int_{t^*}^{t_s}e^{-t/\tau_2}B(v,Z)dt\right]$$

$$\equiv g_4\theta_4+\frac{g_2\tau_2}{\tau_2-\tau_4}(\theta_2+\theta_4)\ ,$$

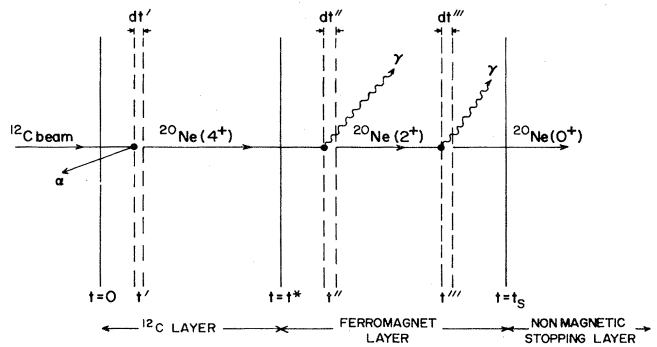

FIG. 8. Schematic of the time sequence corresponding to the creation of the 4_1^+ state and subsequent decay of the 4_1^+ and 2_1^+ states as the ion recoils out of the C target, through the gadolinium layer, and into the stopping foil.

and for the purpose of the calculation,

$$dt=\frac{1}{v}\frac{dE}{dE/dx}$$

and the time integrals are replaced by integrals over the corresponding energies.

The electronic stopping powers tabulated by Northcliffe and Schilling[18] were used in the procedure. The function $B_R(v,Z)$ described by Rutgers parametrization for the transient hyperfine field[11] is used in the integral.

The relationship (displayed in Fig. 7) between these integrals, the field amplitude parameter a, and the experimental precession is given in the following:[17]

$$\Delta\theta(\underline{4_1^+ \rightarrow 2_1^+})_{\text{exp}} = a g_4 \theta_4 ,$$

$$\Delta\theta(\underline{2_1^+ \rightarrow 0_1^+})_{\text{exp}} = a g_2 \theta_2 ,$$

and

$$\Delta\theta(4_1^+ \rightarrow \underline{2_1^+ \rightarrow 0_1^+})_{\text{exp}} = a \left[g_4 \theta_4 + \frac{g_2 \tau_2}{\tau_2 - \tau_4} (\theta_2 + \theta_4) \right] .$$

---

*Present address: Physics Department, Washington College, Chestertown, MD 21620.

†Permanent address: Instituto De Pesquisas Energéticas E Nucleares, São Paulo, Brazil.

[1]K-H. Speidel, G. J. Kumbartzki, W. Knauer, V. Mertens, P. N. Tandon, and N. Ayres de Campos, Phys. Lett. **92B**, 289 (1980).

[2]K-H. Speidel, P. N. Tandon, V. Mertens, W. Trölenberg, G. J. Kumbartzki, N. Ayres de Campos, and M. B. Goldberg, Nucl. Phys. **A378**, 130 (1982).

[3]B. A. Brown, J. Phys. G **8**, 679 (1982).

[4]R. E. Horstman, J. L. Eberhardt, H. A. Doubt, C. M. E. Otten, and G. van Middelkoop, Nucl. Phys. **A248**, 291 (1975).

[5]K-H. Speidel, V. Mertens, W. Trölenberg, M. Knopp, and H. Neuburger, Nucl. Phys. **403**, 421 (1983).

[6]C. Broude, M. B. Goldberg, G. Goldring, M. Hass, M. J. Renan, B. Sharon, Z. Shkedi, and D. F. H. Start, Nucl. Phys. **A215**, 617 (1973).

[7]E. M. Szanto, A. Szanto de Toledo, H. V. Klandor, M. Diebel, J. Fleckner, and U. Mosel, Phys. Rev. Lett. **42**, 622 (1979).

[8]J. M. Brennan, Ph.D. thesis, Rutgers University, 1979 (unpublished).

[9]M. Hass, J. M. Brennan, H. T. King, T. K. Saylor, and R. Kalish, Phys. Rev. C **14**, 2119 (1976).

[10]J. M. Brennan, N. Benczer-Koller, M. Hass, and H. T. King, Phys. Rev. C **16**, 899 (1977).

[11]N. K. B. Shu, D. Melnik, J. M. Brennan, W. Semmler, and N. Benczer-Koller, Phys. Rev. C **21**, 1828 (1980).

[12]K-H. Speidel, G. J. Kumbartzki, W. Knauer, V. Mertens, P. N. Tandon, J. Gerber, and R. M. Freeman, Hyp. Int. **9**, 513 (1981).

[13]A. Becker, A. Holthuizen, A. J. Rutten, C. P. M. van Engelen, and G. van Middelkoop, Hyp. Int. **11**, 279 (1981).

[14]P. C. Zalm, A. Holthuizen, J. A. G. de Raedt, and G. van Middelkoop, Hyp. Int. **5**, 347 (1978).

[15]D. Bazzaco, F. Brandolini, M. DePoli, P. Pavan, C. Rossi-Alvarez, and R. Zannoni, Phys. Rev. C **29**, 1163 (1984).

[16]R. E. Horstman, J. L. Eberhardt, P. C. Zalm, H. A. Doubt, and G. van Middelkoop, Nucl. Phys. **A275**, 237 (1977).

[17]T. Bright, Masters thesis, Rutgers University, 1984 (unpublished).

[18]L. C. Northcliffe and R. F. Schilling, Nucl. Data **A7**, 233 (1970).